Phonons in one-dimensional Peierls-Hubbard systems

L. Degiorgi* and P. Wachter
Laboratorium für Festkörperphysik Eidgenössische Technische Hochschule—Zürich, CH-8093 Zürich, Switzerland

M. Haruki† and S. Kurita
Laboratory of Applied Physics, Faculty of Engineering, Yokohama National University, Hodogaya, Yokohama 240, Japan
(Received 26 February 1990)

Reflectivity measurements from the ultraviolet (UV) down to the far infrared (fir) of one-dimensional mixed-valence Pt-halogen chains are discussed. Particular attention is devoted to the fir spectral range: the relevant one for the study of the phononic properties. We give evidence for the presence of such defects (polarons) along the chain axis, which are manifest in the phonon spectra through the defect modes. A lattice-vibrational calculation is further considered for the discussion of the whole phonon spectra.

I. INTRODUCTION

Recently, the so-called halogen-bridged mixed-valence compounds, which correspond to the chemical formula $[M(\mathrm{en})_2][M(\mathrm{en})_2X_2]Y_4$ [where M=Pt, Pd, or Ni, X=Cl, Br, or I, (en) are amines such as ethylenediamine, and Y are anions such as ClO_4, BF_4, etc.], received a lot of attention from the scientist's community due to their intrinsic low-dimensional properties.[1]

Besides, these one-dimensional compounds are also considered as model or prototype systems for proving the availability of the so-called Peierls-Hubbard theoretical approach. These studies have a lot of implications in the development of theoretical models regarding the new high-T_c superconductors.[2]

The hereafter abbreviated MX compounds are characterized by a skeletal structure consisting of linear chains $\cdots M(\mathrm{II})\cdots X^-\cdots M(\mathrm{IV})\cdots X^-\cdots$ of alternating metal-halogen ions, where the X^- ions are closer to the M(IV) than to the M(II) ions. Along the chain axis (or b axis), each M metal ion is coordinated by four nitrogen atoms of the ethylenediamines. The anions, for instance, ClO_4, then act as glue molecules between the chains, in order to create the three-dimensional single-crystal structure.[1]

Thus, the main structural feature concerns the dimerization of the halogen ions from the midpoint between two nearest-neighbor Pt ions, which follows the appearance of a commensurate charge-density-wave (CDW) ground state. Therefore, these chain compounds are considered to be realized Peierls systems. However, one has to remark that the former dimerized ground state is more complex (since it is more the consequence of the so-called site-diagonal electron-phonon coupling[2]) than the original one considered by Peierls, where the metal atoms positions are dimerized instead of the halogens.

The experimental investigations were mainly devoted to the optical properties of these MX chains.[1,3–5] In the visible energy spectral range the absorption spectra show a very intense additional band, which is ascribed to the charge-transfer (CT) transition between the d orbitals of M(II) and M(IV), respectively.[3] Essentially, this strong absorption, polarized along the chain axis, corresponds to the transition across the Peierls energy gap, formed at the edge of the folded Brillouin zone (BZ) by the dimerization of the halogen X^- ions. Furthermore, Wada *et al.* reviewed the M and X dependence of such a CT band, measuring the polarized reflectivity in the visible energy range.[3]

Besides the CT band, new absorption bands around half the energy of the CT band were detected along the chain axis.[4,5] Of particular interest is the work of Kurita *et al.*, who measured photoinduced absorption spectra of the Pt-halogen compounds at 77 K. By photoexciting across the Peierls gap (i.e., using a He-Ne or Ar laser with photon energy larger than the CT band energy), it is possible to create defects along the chain axis, as a consequence of the electron-hole relaxation to the self-trapped exciton midgap state. These generally correspond to Pt(III) ions, which break down the periodic mixed-valence [i.e., Pt(II) and Pt(IV)] nature in the undoped or ideal chain. Therefore, the absorptions detected below the CT band (i.e., a broad structure at 300 K and three distinct ones at 77 K) are ascribed to the transitions between the midgap levels introduced by the defects and the continuum band.[4–6] The experimental evidence, that such defects should be charged and have a spin, calls for their polaronic nature.[4] It is worth it to remark that the intensity of the midgap absorptions increase linearly with the total excitation light flux and that the photoinduced absorption bands are stable at 77 K and are induced only by light with $\mathbf{E}\|\mathbf{b}$ and are preferentially polarized for $\mathbf{E}\|\mathbf{b}$.[4,6] These last features suggest that the photoinduced defect states are located on individual chains, and not associated with interchain impurities. Furthermore, these photoinduced defects are characterized by their metastable nature, since the spectrum, after having kept the sample at room temperature for some hours after an excitation for 1 h, is equal to the spectrum before any irradiation. This is ascribed to the recombination of the photoinduced defects (i.e., at 300 K the mobility is much

higher than at 77 K). Nevertheless, the appearance of the absorption bands, also before any irradiation, is the evidence of the intrinsic nature of such Pt(III) impurities along the chain axis.[4,5] Besides, the application of an external hydrostatic pressure or the halogen doping (i.e., carried out by exposing the single crystals in a vessel to halogen vapor) are alternative methods to the photoexcitation for creating defects along the chain axis.[7,8] In fact, it is well established that the intragap absorptions originate from the same defect states, whatever the method for the enhancement of their density is.

The experimental evidence that these one-dimensional compounds could support the presence of defects (intrinsic or induced) along the chain axis motivated our further investigations in the far-infrared energy range. The main aim consists in finding the signature of such defects within the phonon spectrum.

In a previous work on the ir-active phonon modes we proposed a first tentative assignment of the structures, measured along the chain axis, with the help of a phenomenological lattice-vibrational calculation.[5] With the present work we will completely review the fir spectrum of the whole Pt-halogen series and above all, we will enlarge our phenomenological analysis to the case of a one-dimensional chain containing Pt(III) defect sites. We will give, therefore, the optical evidence of the existence of the localized mode, as a fingerprint of the defects.

II. EXPERIMENT AND RESULTS

The reflectivity [$R(w)$] measurements have been obtained using four different spectrometers in order to cover the whole range of energies between 1 meV and 12 eV. Such measurements were performed with light polarized parallel and perpendicular to the chain axis of our large single crystals ($2\times1\cdot5\times1$ mm^3) of the whole Pt-halogen series and with temperature dependence between 300 and 6 K. In the fir we have made use of a Fourier spectrometer (with an energy resolution of 1 cm^{-1}) with a triglicyne sulfate detector down to 25 cm^{-1} and with a He-cooled Ge bolometer from 100 to 8 cm^{-1}. It is worth it to remember, furthermore, that all optical functions [e.g., $\epsilon(w)$ or $\sigma(w)$] can be obtained through Kramers-Kronig transformations of the $R(w)$ data.

In order to perform $R(w)$ measurements in the fir after photoexcitation of the sample, we have implemented a device on the Fourier spectrometer. In fact, it consists of a special N_2 cryostat, which permits us to photoexcite the sample with a laser at 77 K for a desired time. The He-Ne lasers we used had a minimal power between 0.1 and 0.2 mW and they irradiated red (633 μm) and green (544 μm) light, respectively (i.e., in the energy spectral range of the CT band). For more details, concerning the experimental setup and the crystal growth procedure, we refer the reader to the literature.[9]

Here, we will now present the experimental results relative to the fir energy range, which, indeed, is the relevant one for the discussion of the phonon modes. Figure 1 shows the $R(w)$ spectra along the chain axis for the whole Pt-halogen series at 6 K. These spectra are characterized by five highly polarized structures (N.B. for the Pt-I on the top of the figure, these are marked with arrows and the measurements on Pt-Br were performed on new, better, single crystals than those of Ref. 5). For a complete overview about the optical response of the Pt-halogen chains between the fir and UV energy spectral range we refer the reader elsewhere in the literature and to our recent works.[5,9]

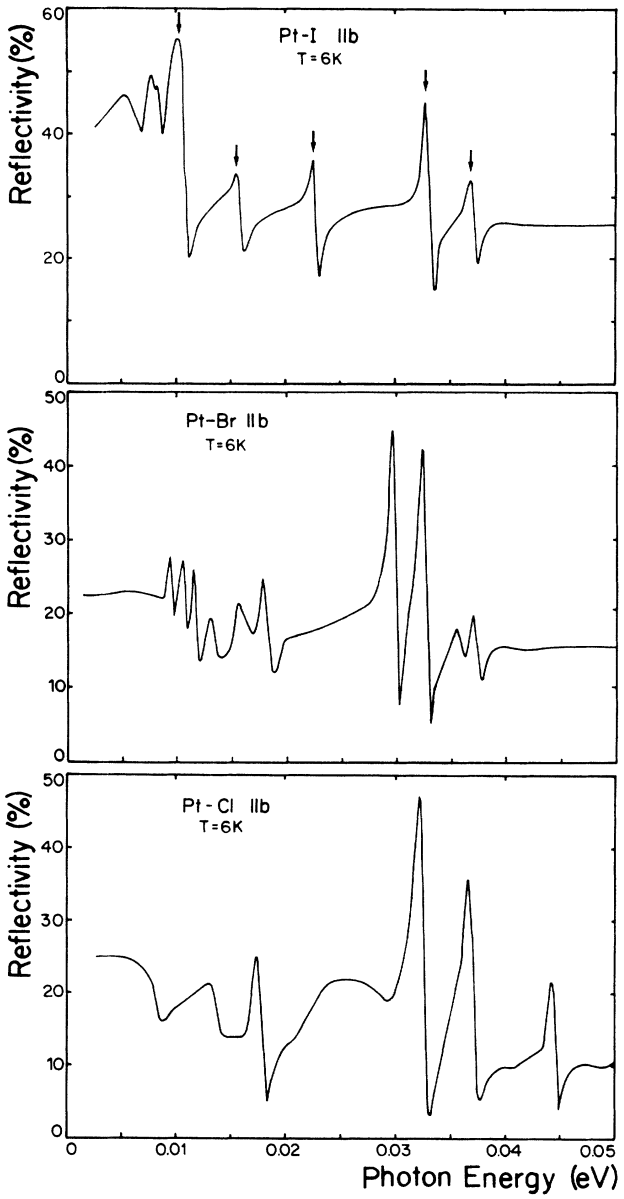

FIG. 1. fir-$R(w)$ at 6 K for the whole Pt-halogen series along the chain axis.

III. DISCUSSION

As pointed out in the previous section, the common features which characterize the $R(w)$ spectra of the three investigated Pt-halogen compounds concern, above all, the five highly polarized mode structures along the chain axis. The present discussion will be devoted to the interpretation of these phonon modes through the help of a phenomenological lattice-vibrational calculation.

A. Phenomenological lattice-vibrational calculation

To get quantitative insight into the internal phonon modes, we will propose a phenomenological lattice-vibrational calculation based on the linear harmonic approximation. We will develop the calculation formalism following the approach of Barker and Sievers.[10] In our previous work[5] we have introduced a model phonon calculation for the case without defects, starting with the crystallographic equivalence of our chains with the three-dimensional isotropic perovskite structure of the $BaPb_xBi_{1-x}O_3$ compound. Here, we will first overview the basic features and enlarge the procedure to the case with defect sites.

We take our Pt-halogen compounds as a one-dimensional two-atom base chain. From the CDW ground state the dimerized unit cell Pt(III$+\delta$)—X^-—Pt(III$-\delta$)—X^- follows (where $0<\delta<1$ describes the charge disproportionation), which contains four atoms along the chain. Next, an (en) planar molecule is attached to each Pt ion. These bonds are modeled by four out-of-chain bendings where each of them is formed by a complex with the total mass of C and N. Thus, the unit cell of the undoped Pt-halogen chain looks like the situation of Fig. 10 in Ref. 5, which contains a total of 12 atoms. Of course, this could be understood as the consequence of the dimerization along the chain axis due to the CDW ground state; furthermore, a folded Brillouin zone also follows.

In order to calculate the vibrational modes in the linear harmonic approximation, we consider two types of nearest-neighbor interactions: the in-chain stretching distortions with the spring force constants K_i and the out-of-chain bending distortions with the spring force constants K_i', where $i=1,2$, indicates the Pt ions with $3+\delta$ and $3-\delta$ charge disproportionation, respectively. The mixed-valence nature of these two atomic base chains is thereupon renormalized within the spring force constants K_i and K_i'.[5]

So far, only the undoped chain was considered. However, from the former introduction it is well known that these linear chains could support the presence of defects. Of course, their presence will influence the Raman and the ir phonon spectrum as well.

From a general point of view, introducing a defect in our Pt-halogen chains consists in creating a new local charge disproportionation. In other words, there is a new charge distribution, which breaks down the periodic mixed-valence nature of the undoped chain.

In order to visualize a concrete example, we will consider hereafter, the case of a polaron defect. It is manifest by the presence of Pt(III) ions, which locally incorporate the new charge disproportionation.

Thus, in our phenomenological calculation the new charge distribution is considered by new spring force constants (K_3 and K_4) around the Pt(III) ions. Figure 2 summarizes the situation of a Pt-halogen chain without and with the polaron defect (for the sake of clarity the amines complex with the out-of-chain bending interactions are not shown).[11]

We postulate that the defect is confined within the two

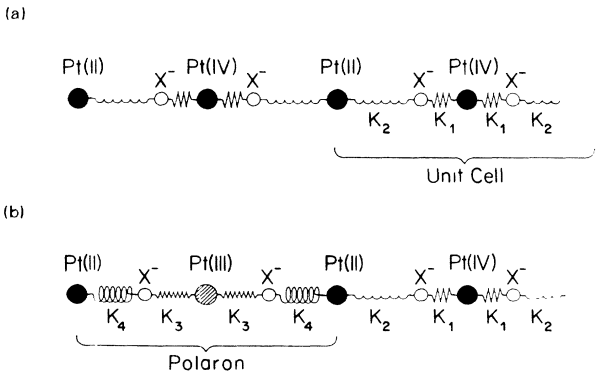

FIG. 2. MX-chain (a) without and (b) with the polaron defect used for the fit.

adjacent Pt-halogen units. Of course, this choice strengthens the localization of the defect (and also of the corresponding phonon mode, see below) but limits the number of new parameters in the calculation. However, the localization or the short range of interaction of the defect is also established well by the theoretical work of Baeriswyl and Bishop, at least in the strong electron-phonon coupling case.[12] Within their approach, based on the Peierls-Hubbard tight-binding Hamiltonian, they observed that only the electronic states (ϵ_n) of the nearest-neighbor Pt ions to the defect are affected by the presence of a polaron.

Concerning the vibrational response at $\mathbf{k}=0$, besides the ir-active modes (i.e., zone boundary acoustic, the stretching, and the ir-active bending mode[5]), the presence of the defect along the chain axis introduces new phonon modes in the spectrum. The situation is very similar to the case of a chain of alternating masses m_1 and m_2 ($m_1<m_2$), when an isotope substitution happens.[10] If the substituted mass m' is smaller than m_1, a so-called localized mode appears; however, if m' is larger than m_1 (i.e., heavy isotope substitution), a new mode arises between the optic and the acoustic phonon band. In the last case, the localized mode is called a gap mode. A single localized mode is also obtained in the case of isotope substitution for the mass m_2.[10]

For our Pt-halogen chains, the localized mode around the defects arises in the linear chain by reducing the force constants on each side of one atom [Fig. 2(b)]. In order to fix the idea, it is useful to define a factor γ as $1-K'/K$, which describes the strength of the spring force constant substitution K' for K (i.e., for our present considerations we take into account a simplified configuration where the lattice interactions are described by the unique spring force constant K and around the defect by substituting K with a new spring force constant K'). It follows that for $\gamma<1$ ($0<\gamma\leq 0.8$), the localized mode is essentially a gap mode and for $\gamma\rightarrow 1$, the former mode decreases in frequency then changes its character and enters the acoustic band. Once within the acoustic band, there is a group of eigenvectors or modes which have a large amplitude near the impurity. Such a group of modes is called a "resonant mode."

Hereafter, since the defect situation in our systems will always correspond to the gap mode regime, we will briefly use the expression of a localized mode.

Our interest lies mainly in the zone-center ($\mathbf{k}=0$) modes of the folded Brillouin zone because they are relevant for the ir spectra. Therefore, following our previous work,[5] one has to build up the dynamical matrix (D_{ij}) for the two situations of Fig. 2 (i.e., without and with defect) at $\mathbf{k}=0$ by writing down the equation of motion in a one-dimensional space. Considering the linear harmonic approximation, one obtains the matrix (A2) of Ref. 5 in the case without defect, and for a chain with a defect [Fig. 2(b)] we refer the reader to the enclosed Appendix. Solving the corresponding determinantal equation through the diagonalization of D_{ij} (Ref. 5) we determine the eigenvalues w_n of the ir-active and of the Raman modes as well, and afterwards the corresponding normal modes.

Of course, the dynamical matrix D_{ij} has been built up within the unit cell with the use of cyclic boundary conditions. Furthermore, if we consider a unit cell of 144 atoms (i.e., which corresponds to an even number of undoped unit cells, namely 12), we have to diagonalize a 144×144 dynamical matrix and we would then obtain for the case without defect the phonon dispersion relation $w(k)$ for 12 points between $-\pi/2a$ and $\pi/2a$ (a is the Pt-X lattice constant in the ideal metal chain, i.e., the undimerized chain).[10] In fact, the diagonalization of the 144×144 D_{ij} matrix at $\mathbf{k}=0$ for the situation of Fig. 2(a) is equivalent to the eigenvalues problem solution within a 12-folded Brillouin zone.

The calculation of the vibrational modes in the presence of impurities is performed on a unit cell of N atoms with one defect. It is clear that the size of the unit cell, which, by the way, corresponds to the new unit cell of the doped chain, is related to the impurity concentration. In fact, due to the cyclic boundary conditions, the chain contains one defect or impurity for each N atom [N.B., then the $N\times N$ D_{ij} matrix must be diagonalized (see the Appendix)]. Thereupon, the impurity-mode strengths scale directly with the concentration. Consequently, the larger the concentration of impurities is, the stronger the localized mode appears and reduces the strength of the original lattice absorption, since its strength is "borrowed" by the impurity modes.[10] Furthermore, the entire acoustic and optic bands have become active in the fir absorption due to the folding of the BZ.

Up to now, we considered the consequence of the presence of defects only on the phonon modes along a simple one-dimensional chain. However, since we take into account the out-of-chain bending interactions, also another localized mode is expected along the chain axis, due to the new spring force constants distribution around the defect. Similar to the gap mode described above, this additional localized mode has similar properties relative to its strength and localization. Hereafter, we will call it the localized bending mode.

Before concluding this subsection, we would like to recall the attention of the reader to the effect of the impurity on the out-of-chain lattice interactions also. In fact, we have previously taken into account the effect of its presence on the intrachain lattice interactions. Therefore, besides the new spring force constant distribution along the chain axis, new out-of-chain bending force constants (K_5) must be introduced around the defect within the phenomenological calculation. In the next subsection, we will apply this phenomenological approach to our Pt-halogen chains, in order to interpret the phonon spectra along the chain axis.

B. ir and Raman active phonons in the Pt-halogen chains

The application of the phenomenological lattice-vibrational calculation consists in finding the best set of parameters K_i and K_i', in order to obtain the best possible fit with the experimental data.

In Table I we summarize the spring force constants used in the calculation and for which the best fit is obtained. An interesting feature evolves immediately from Table I; namely, the tendency to reach the best fit with in-chain spring force constants K_1 and K_2, which do not appreciably differ from each other. This is more and more pronounced going from Pt-Cl to Pt-Br and to Pt-I. The progressive leveling of K_1 and K_2 is in contrast to the numerical conclusions proposed by Clark, who considered only the interactions within the chain [i.e., with $K_i'=0$ the dynamical matrix reduces its dimension to four and would correspond to the 4×4 matrix without defects (see the Appendix of Ref. 5)], and where K_1 differs about a factor between 10 and 20 from K_2.[1] We have claimed that this large difference is to be ascribed to a certain renormalization due to the omission of the out-of-chain bending interactions. However, the small and increasing (from Pt-I to Pt-Cl) difference between K_1 and K_2 in our fit accounts for the δ charge disproportionation on the Pt site.[5]

Concerning the spring force constants (K_3 and K_4) around the defect, these are approximately a factor 2 less than K_1 and K_2. Baeriswyl and Bishop calculated that the lattice dimerization around the Pt(III) ion (i.e., the defect) is only half the normal dimerization.[12] In fact, around the defect there is a weak-coupling limit as a consequence of the reduced-charge disproportionation

TABLE I. Spring force constants K_i and K_i' (with $i=1,2$) and K_3, K_4, and K_5 used in the phenomenological fit.

	K_1	K_2	K_1'	K_2'	K_3	K_4	K_5 (mdyn/Å)
Pt-Cl	1.10	0.87	0.66	0.02	0.50	0.40	0.50
Pt-Br	0.80	0.70	0.58	0.06	0.40	0.35	0.45
Pt-I	0.73	0.61	0.66	0.01	0.40	0.30	0.50

and, consequently, screening of the lattice interactions arises, so far supporting the reduced values of K_3 and K_4.

The results of our fitting procedure for the ir-active phonon modes is presented in Table II, which furthermore shows the good agreement between the experimental and the calculated modes. We would like to remind the reader that we expose the eigenfrequencies (calculated and experimental) for each Pt-halogen compound in increasing order of energy and that the temperature dependence of the frequency is negligible.

The differences between the calculated and the experimental values generally oscillate between 0.5 and 3 meV. Different valence delocalizations could arise in domains along the chain characterized by different halogen dimerizations. Then it was claimed that similar effects could be the origin of the small dispersion of the ir modes.[5]

The assignment of the phonon modes is obtained by the calculation of the eigenstates. The fit procedure was applied for the undoped and for the doped Pt-halogen chain as well. In fact, in the following figures the eigenstates in the two situations for the Pt-Cl chain are compared. We depict, with the vertical bars, only the ionic movements or displacements along the chain axis, omitting for clarity the corresponding components of the (en) complexes and also the dimerization of the halogen ions.

Firstly, the eigenstate of the lowest-frequency (i.e., at 17, 12, and 11 meV for Pt-Cl, Pt-Br, and Pt-I, respectively) ir mode is shown in Fig. 3. It corresponds to the zone-boundary acoustic mode, which is expected, since the reduced mass of this mode is equal to the Pt-ion mass. As it will be the case for all other ir modes, the eigenvalues are not at all affected by the presence of defects which, however, strongly influence the eigenstate around the defects itself.

Figure 4 shows instead the other typical ir mode for a one-dimensional chain; namely, the stretching phonon mode which is at 44.5, 28, and 23 meV for Pt-Cl, Pt-Br, and Pt-I, respectively.

The phonon states at 36.5 meV for Pt-Cl and at 37 meV for Pt-Br and Pt-I are assigned to the ir-active bending mode. This is induced by the out-of-chain bending interactions and is depicted in Fig. 5.

So far, we have discussed the ir-active phonon modes, characterizing each one-dimensional chain with the unit cell shown in Fig. 10 of Ref. 5 (i.e., without defect). However, the presence of polarons along the chain axis

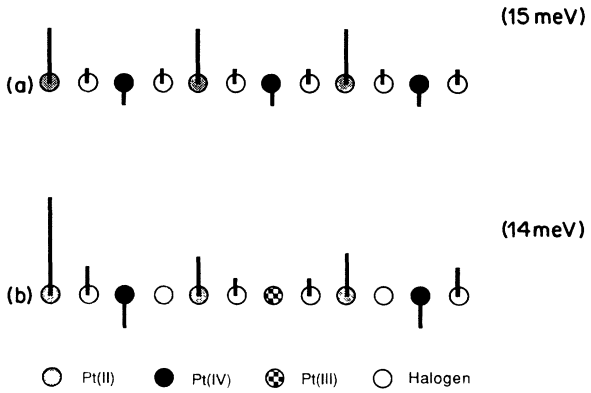

FIG. 3. Eigenstate of the acoustic mode for the Pt-Cl chain (a) without and (b) with a polaron defect (within brackets, the calculated eigenvalue).

[Fig. 2(b)] introduces also the so-called localized mode besides the changes described above for the former phonons (see Figs. 3–5).

The new spring force constant distribution around the defect (K_3 and K_4) is responsible for the localized gap mode at 25, 18, and 16 meV for Pt-Cl, Pt-Br, and Pt-I, respectively. The corresponding eigenstate of Pt-Cl (Fig. 6) demonstrates well its localization. We have just mentioned in the previous subsection that this strong localization is a direct consequence of the small coherence length of the defect and then, of the limited range of the new spring force constant distribution (i.e., up to the adjacent Pt-X cell).

In addition, we find, in our calculation, another localized mode which is induced by the presence of the out-of-chain bending interactions; namely, the so-called localized bending mode (Fig. 7). This last mode is then assigned to the fifth structure in the phonon spectra at 32 meV for Pt-Cl, and at 33 meV for Pt-Br and Pt-I. However, in a previous work we have assigned it to an ir mode of external type.[5] In fact, it was argued that this external mode involves the whole Pt-X chain against the interchain complexes formed by the (ClO_4) molecules. Besides, the fact that the reduced mass of this external mode is essentially equal to the total mass of the (ClO_4) molecule for the whole Pt-halogen series, could also support the experimental evidence of finding the external

TABLE II. Experimental and calculated fir phonon frequencies (w_n) (N.B., w_n are exposed in increasing order of energy).

		w_1	w_2	w_3	w_4	w_5 (meV)
Pt-Cl	expt.	17.0	25.0	32.0	36.5	44.5
	calc.	14.0	26.0	34.0	35.0	44.0
Pt-Br	expt.	12.0	18.0	28.0	33.0	37.0
	calc.	14.6	17.0	24.0	32.0	37.0
Pt-I	expt.	11.0	16.0	23.0	33.0	37.0
	calc.	11.0	14.0	20.0	33.0	39.0

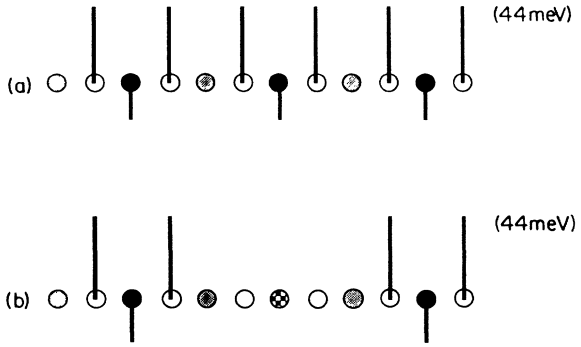

FIG. 4. Eigenstate of the stretching mode for the Pt-Cl chain (a) without and (b) with a polaron defect (within brackets, the calculated eigenvalue).

mode at the same frequency for all Pt-X compounds. Nevertheless, with the described phenomenological approach we can only consider the so-called internal modes, and the last hypothesis is beyond such an approach and remains an alternative explanation.

Besides the ir-active phonon modes, the diagonalization of the dynamical matrix D_{ij} also offers us the Raman modes; namely, the Raman breathing and bending modes. In Table III the experimental data concerning those modes are compared with the corresponding calculated ones.

Concerning the Raman bending mode, we should remind the reader that, for the linear chain without defect, a seven-times degenerate mode is obtained at approximately 26 meV. Actually, this degeneracy will be removed by the presence of defects [i.e., from the model calculations point of view by the K_5 spring force constant around Pt(III)], which essentially split the degenerate states in two parts. However, the calculated split results in the range of ~ 4 meV for our choice of K_5.

The calculated Raman bending mode agrees very well with the experimental result of Tanino *et al.*, who measured the Raman spectra of mixed-halogen compounds Pt-$(Cl_{1-x}Br_x)$.[13]

The halogen independence of these degenerate modes follows from the fact that only the (en) complexes are involved but the Pt and halogen ions do not move at all. The eigenvalue calculation demonstrates this fact well since the Raman bending mode frequencies depend only on K_i' and K_5 (i.e., which are affected by the valence on the Pt ions). Besides, the numerical values of the K_i' and K_5 constants are quite the same for the whole Pt-halogen series (Table I). The small differences account again for the different δ disproportionation on the Pt ions and consequently for the small experimental dispersion of these bending modes. However, from the experimental point of view, the resolution is not enough in order to detect such a dispersion and the further splitting of about 4 meV due to the defects.[13]

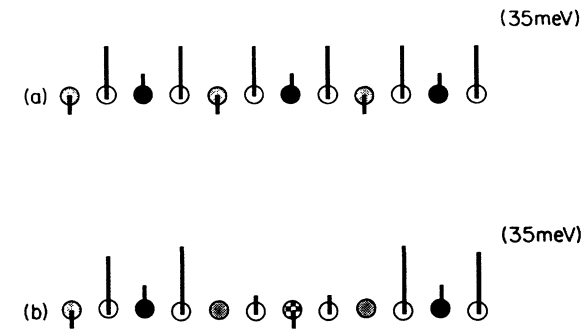

FIG. 5. Eigenstate of the ir-bending mode for the Pt-Cl chain (a) without and (b) with a polaron defect (within brackets, the calculated eigenvalue).

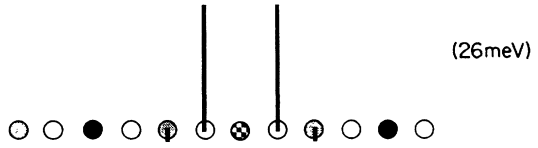

FIG. 6. Eigenstate of the gap mode for the Pt-Cl chain with a polaron defect (within brackets, the calculated eigenvalue).

Regarding the Pt-I compound, we did not find any published experimental results for the corresponding Raman bending modes. Nevertheless, from the above considerations about the halogen independence, an experimental frequency of about 26 meV is expected, as predicted by our calculation. In fact, preliminary Raman measurements point out a mode around 23 meV.[14] An investigation of Pt-$(Cl_{1-x}I_x)$ would be needed in order to prove the halogen independence of this mode.[13]

Returning now to the Raman breathing mode, we depict first of all the corresponding eigenstate in Fig. 8. In addition, regarding this Raman mode, the most interesting experimental evidence concerns the fine-splitting effect of this mode and of its overtones. Through resonant Raman measurements Tanaka *et al.* resolved the Raman mode into five structures with three main components.[15,16] Firstly, they proposed the halogen isotopic splitting as a possible explanation of the fine structures. Nevertheless, the expected frequency split in the breathing mode for different halogen isotopes is larger than the measured one. Thus, they conclude that the most probable origin of the fivefold split is to be ascribed to the presence of different domains composed by short chains of different length.

With a similar investigation of the Pt-Br compound, Conradson *et al.* also claimed that the presence of defects could be a further cause for the five structures of the

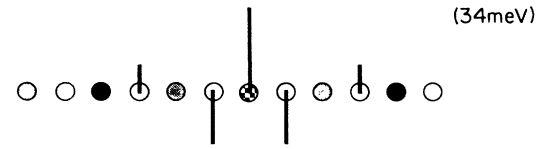

FIG. 7. Eigenstate of the localized bending mode for the Pt-Cl chain with a polaron defect (within brackets, the calculated eigenvalue).

TABLE III. Experimental and calculated frequencies of the Raman modes (breathing and bending mode).

		Pt-Cl	Pt-Br	Pt-I (meV)
$w_{\text{breathing}}$	expt.[a]	38.4	21.5	15.4
	calc.	38.4	22.3	17.1
w_{bending}	expt.[b]	26.0	26.0	
	calc.	22.8–26.2	22.6–25.3	22.6–25.9

[a]Reference 1.
[b]Reference 13.

Raman breathing mode.[17] This seems to find a confirmation in our lattice-vibrational calculation. In fact, besides the Raman and ir modes described above, many other modes at the Γ point of the BZ are obtained. Among these, many modes have a Raman symmetry and eigenfrequencies around the breathing mode, even though the frequency split (i.e., around 1.7–2.3 meV) is much larger than the experimental one (around 0.5 meV). Moreover, a particular interest is assumed by that Raman mode which has a breathing symmetry and is strongly localized around the defect (i.e., a polaron). Within our phenomenological calculation it should appear at approximately 27, 15, and 11 meV [i.e., at a frequency about a factor $(\sqrt{2})^{-1}$ less than the normal breathing Raman mode frequency] for Pt-Cl, Pt-Br, and Pt-I, respectively. For Pt-Cl the frequency is equal to the Raman bending mode. Therefore, the mode detected around 26 meV could be the contribution of two Raman active phonons (i.e., the bending and the localized breathing one). Recent preliminary Raman measurements on Pt-I clearly give the evidence of a shoulder around 14 meV superimposed to the Raman breathing mode at 15.4 meV of the undoped chain. Furthermore, similar measurements on the heavy-doped Pt-I compound [i.e., with approximately 5 mol. % of Pt(III) along the chain axis] confirm the energy shift of the breathing mode.[14] It is important to realize that the squared eigenfrequency of the Raman defect mode is equal to $(K_3+K_4)/M_{\text{halogen}}$ [the corresponding eigenfrequency by the undoped chain is $(K_1+K_2)/M_{\text{halogen}}$, thus a factor 2 larger than the former one] and consequently, by increasing the density of such Pt(III) sites, this last mode will be dominant. For the Pt-Br compound, however, we do not know enough accurate Raman measurements which could prove and confirm this guess from our lattice-vibrational calculation.

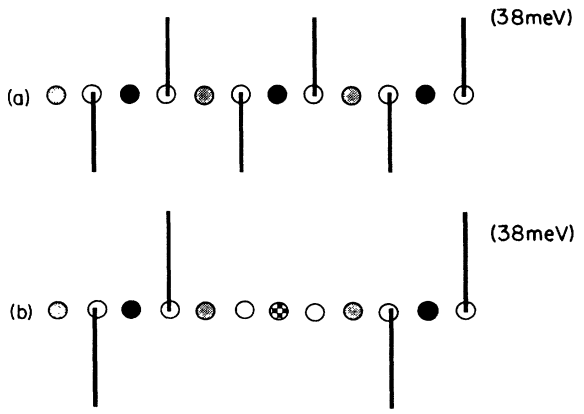

FIG. 8. Eigenstate of the Raman breathing mode for the Pt-Cl chain (a) without and (b) with a polaron defect (within brackets, the calculated eigenvalue).

All these modes at the Γ point of the BZ arise as consequence of the BZ folding caused by the presence of defects. Then, the defect density determines the large size of the unit cell where the phenomenological calculation is carried out. Since a sum rule is considered for the total mode strength, it happens that the total strength of the normal one-dimensional modes (i.e., for a chain without defects) is borrowed by the impurity modes.

With high defect concentration (i.e., small unit cell), a corresponding small amount of modes at the Γ point of the BZ is expected. These, on the contrary, will have a considerable mode strength. The intrinsic concentration of defects in our Pt-halogen chains amounts to approximately 1 mol % which corresponds to one defect in each 100 unit cells.[18] Although this gives sizable normal and impurity modes, all the other Γ point modes are at least a factor 10 smaller in strength. Concerning the ir-active mode, our calculation with the presence of defects gives evidence of new ir modes at very low frequencies (i.e., below the zone-boundary acoustic mode) and at frequencies smaller than the stretching mode. This explains the structures at very low frequencies, the splitting of the zone-boundary acoustic mode, and the broad asymmetric shape of the stretching mode detected along the chain axis (see Fig. 1).

As briefly mentioned in the previous section about the experimental setup, we also tried to measure the photoinduced phonon spectrum for the whole Pt-halogen series. This was performed with the aim to artificially change the defect concentration. Following the experimental procedure of Kurita *et al.*,[4] we measured in the fir the $R(w)$ spectra along the chain axis after photoexcitation with a laser light at an energy above the CT band absorption energy for different periods of irradiation. We did not obtain any difference in the phonon spectra before and after the photoexcitation. Of course, it is possible that the laser power is not enough to pump a large amount of impurities. However, this negative result also claims that the intrinsic amount of defect is just considerable and it could not be further improved by photoexcitation.

In other words, the augmented concentration is not large enough in order to alter the impurity phonon mode strength. Even though it is very difficult to characterize the samples regarding their impurity concentration, it is established quite well that the intrinsic amount is therefore about 1 mol %, not far away from the saturation point of approximately 4–5 mol %.

Besides, we measured many doped compounds with nominal different impurity concentrations.[18] In this case also, the spectra did not change at all, confirming the difficulty of finding the fingerprint of the defect concen-

tration dependence in the fir optical measurements. Once again, it seems to us that, besides the objective difficulty in characterizing the defect concentration of the samples, this intrinsic impurity concentration should be, nevertheless, near the saturation point.

Before concluding, we will discuss some further aspects concerning the phenomenological calculation. A first aspect, which was taken into account during the lattice-vibrational calculation, concerns the distribution of the defects within the unit cell. It was proved that, due to the strong localization and the cyclic boundary conditions, the position of the polaronic defect within the chain axis is not influential on the phonon modes. Besides, the experimental results and the agreement with the phenomenological calculation claim further that the defects are uniformly distributed along the chain. The contrary would indeed correspond to a random distribution which also implies, from a phenomenological point of view, a random distribution of the spring force constants (since there would exist different domains with different charge distributions and consequently lattice interactions). Then, as demonstrated well by Barker and Sievers,[10] the phonon spectrum would not be characterized by well-defined mode structures, but on the contrary by broad and/or "washed-out" phonons.

Moreover, the calculations were performed paying attention to the so-called charge neutrality. The unit cell always contained an electron-hole pair of defects (i.e., hole and electron polaron). Also in this respect such a dependence does not affect the above conclusions.

Another important aspect regards the type of the defect. Up to now, the phenomenological fit to the experimental data was performed for the case of a polaron defect. Nevertheless, a big debate arose recently about the identification of the defect type (i.e., polaron or soliton). In fact, Kuroda *et al.*[8] and Sakai *et al.*[19] although obtaining results similar to those of Kurita *et al.*,[4] extrapolated another conclusion from the analysis of their data, based on the presence of neutral soliton defects. Therefore, the same calculation was performed for other kinds of impurities; namely, for the neutral and charged solitons, for which similar results to the previous ones for the polaron case were achieved. The defect dependence concerns only the symmetry of the corresponding eigenstates and, among them, that of the localized impurity in particular. This is directly related to the spring force constant distribution which depends on the charge distribution modeling the defect. We would like to remember that the choice of the spring force constant distribution (which appears in Figs. 9 and 10) is related, as by the polaron

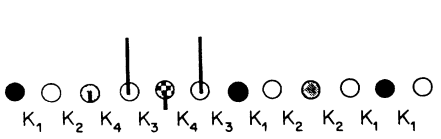

FIG. 9. Eigenstate of the localized gap mode for the Pt-Cl chain with a neutral soliton; please note the spring force constants distribution used for the fit (within brackets, the calculated eigenvalue).

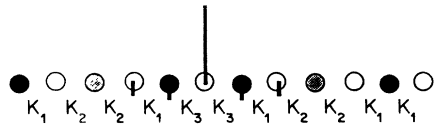

FIG. 10. Eigenstate of the localized gap mode for the Pt-Cl chain with a positive charged soliton; please note the spring force constants distribution used for the fit (within brackets, the calculated eigenvalue).

case, to the halogen dimerization around the defect. The halogen displacements were calculated with the PH model of Baeriswyl and Bishop (see Figs. 10 and 11 of Ref. 12). For example, by the charge soliton (Fig. 10) the halogen between the two Pt(IV) ions (which actually represent the defect) is completely undimerized. This local perturbed configuration is modeled by the symmetric spring force constant (K_3) distribution around the former undimerized halogen ion. Then, from the nearest-neighbor Pt-halogen unit on (along the chain axis) the configuration looks like the unperturbed chain, which we further model with K_1 and K_2. In Figs. 9 and 10 the localized modes for the case of a neutral and charged soliton in the Pt-Cl compound are presented, respectively. Also, for these defects, the strong localization of the impurity mode appears clearly. The calculations were performed using the same spring force constants of Table I. It follows that the type of the impurity has a marginal importance in the above conclusions. From the optical point of view it is not possible to distinguish between different defects but one has to combine other experimental methods. For the present situation, we have pointed out that the impurities should simultaneously have a charge and a spin, which, however, is not the case for the solitons.

Finally, we would like to remember that by applying the Peierls-Hubbard model of Baeriswyl and Bishop,[2,12] where our fitted spring force constants are considered as input parameters, it was possible to find a link between the phononic properties, the electronic ones and, above all, the static distortion characterizing the dimerized CDW ground state.[5] This was an evidence, at least indirect, of the intrinsic physical consistency of the K parameters used for the vibrational calculation (i.e., they did not have a numerical meaning only).

IV. CONCLUSION

Our thorough optical measurements between UV and down to the fir give the evidence of the presence of defects along the chain axis of the one-dimensional Pt-halogen compounds. Discussing with particular emphasis the fir spectra, we found the signature of the impurities within the phonon spectra by detecting the defect ("localized") modes. Our conclusions are well confirmed and supported by the lattice-vibrational calculation based on the linear harmonic approximation. Even though the optical investigations alone are not enough for discerning between the type of the defects, we pointed out their probable polaronic nature.

Lastly, we would like to point out the similarity of our

Pt-halogen chains with the polyacetylene systems. In fact, roughly speaking, these two systems belong to the same category in the sense they have the twofold degeneracy and can therefore support the defect (as, e.g., solitons). Onodera first suggested the consistency of different theoretical approaches, concerning these compounds, within the continuum limit[20] (the reader can find an extended discussion elsewhere, e.g., in Ref. 9) that afterwards permits us to establish a universal behavior of these similar one-dimensional systems. Then, our Pt-halogen compounds could be considered as another prototype class of one-dimensional compounds, which can be suitably studied from the theoretical and experimental point of view, as well.

ACKNOWLEDGMENTS

The authors are grateful to Dr. D. Baeriswyl, Dr. R. Monnier, and Dr. A. R. Bishop for stimulating discussions and to E. Jilek, J. Müller, and H. P. Staub for technical assistance.

APPENDIX

We present here the dynamical matrix D_{ij} for a one-dimensional Pt-halogen chain with a polaron defect (see Fig. 2). Actually, we enlarge the matrix D_{ij} as developed for the case without defect in the Appendix of Ref. 5. We consider a unit cell formed by 12 ions along the chain, where each Pt ion is coordinated by four bonds of the (en) molecule. The defect [i.e., a Pt(III) ion] is located on site number 5. It results in a 36×36 D_{ij} matrix which has the following general and schematic form:

$$D_{ij}=\left[\begin{array}{c|c} H & \tilde{H} \\ \hline \tilde{H} & H' \end{array}\right]$$

(1.....12 / 13.....36)

[N.B., i and j number, from 1 to 12, the Pt and X ions along the chain alternatively [Pt(III) on site 5] and from 13 to 16 the four (en) bonds to the Pt site 1, from 17 to 20 to Pt site 3 and so on up to 36], where the 12×12 matrix H_{ij} is (N.B., we write only the matrix elements which differ from zero)

$$H=\begin{bmatrix}
H_1 & -K_1 & 0 & & & & & & & & 0 & -K_1 \\
-K_1 & H_2 & -K_2 & & & & & & & & & \\
0 & -K_2 & H_3 & -K_4 & & & & & & & & \\
 & & -K_4 & H_4 & -K_3 & & & & & & & \\
 & & & -K_3 & H_5 & -K_3 & & 0 & & & & \\
 & & & & -K_3 & H_4 & -K_4 & & & & & \\
 & & & & & -K_4 & H_3 & -K_2 & & & & \\
 & & & 0 & & & -K_2 & H_2 & -K_1 & & & \\
 & & & & & & & -K_1 & H_1 & -K_1 & & \\
 & & & & & & & & -K_1 & H_2 & -K_2 & \\
 & & & & & & & & & -K_2 & H_6 & -K_2 \\
0 & & & & & & & & & & -K_2 & H_2 \\
-K_1 & & & & & & & & & & &
\end{bmatrix}$$

with the diagonal elements $H_1=2K_1+8K_1'$, $H_2=K_1+K_2$, $H_3=K_2+K_4+8K_2'$, $H_4=K_3+K_4$, $H_5=2K_3+8K_5$, and $H_6=2K_2+8K_2'$.

Then, the diagonal 24×24 matrix H_{ij}' has the following form:

$H_{ii}'=K_1'+K_2'$ for i from 13 to 20 and from 29 to 36 ,

$H_{ii}'=K_2'+K_5$ for i from 21 to 28 ,

$H_{ij}'=0$ for all $i\neq j$ (i,j from 13 to 36) .

Finally, the 12×24 matrix $\tilde{H}_{ij}$ takes the values

$\tilde{H}_{1j}=-K_1'$ for j from 13 to 20 ,

$\tilde{H}_{3j}=-K_2'$ for j from 17 to 24 ,

$\tilde{H}_{5j}=-K_5$ for j from 21 to 28 ,

$\tilde{H}_{7j}=-K_2'$ for j from 25 to 32 ,

$\tilde{H}_{9j}=-K_1'$ for j from 29 to 36 ,

$\tilde{H}_{11j}=-K_2'$ for j from 13 to 16 and from 33 to 36 ,

all other $\tilde{H}_{ij}=0$ (for i from 1 to 12 and j from 13 to 36) .

In conclusion, the reader should pay attention to the fact that the charge neutrality was not considered here.

*Present address: Department of Physics and Solid State Science Center, University of California Los Angeles, Los Angeles, California 90024.

†Present address: Laboratorium für Festkörperphysik ETH-Zürich, CH-8093 Zürich, Switzerland.

[1]R. J. H. Clark, in *Advances in Infrared and Raman Spectroscopy,* edited by R. J. H. Clark and R. E. Hester (Wiley, New York, 1984), Chap. 3, p. 95, and references therein.

[2]D. Baeriswyl and A. R. Bishop, Phys. Scr. **T19A**, 239 (1987).

[3]Y. Wada, T. Mitani, M. Yamashita, and T. Koda, J. Phys. Soc. Jpn. **54**, 3143 (1985).

[4]S. Kurita, M. Haruki, and K. Miyagawa, J. Phys. Soc. Jpn. **57**, 1789 (1988).

[5]L. Degiorgi, P. Wachter, M. Haruki, and S. Kurita, Phys. Rev. B **40**, 3285 (1989).

[6]R. J. Donohoe, S. A. Ekberg, C. D. Tait, and B. I. Swanson, Solid State Commun. **71**, 49 (1989).

[7]M. Haruki and S. Kurita, Phys. Rev. B **39**, 5706 (1989).

[8]N. Kuroda, M. Sakai, Y. Nishina, M. Tanaka, and S. Kurita, Phys. Rev. Lett. **58**, 2122 (1987).

[9]L. Degiorgi, Ph.D. thesis, Eidgenössische Technische Hochschule, Zurich, 1990.

[10]A. S. Barker, Jr. and A. J. Sievers, Rev. Mod. Phys. **47**, S1 (1975).

[11]L. Degiorgi, M. Haruki, P. Wachter, and S. Kurita (unpublished).

[12]D. Baeriswyl and A. R. Bishop, J. Phys. C **21**, 339 (1988).

[13]H. Tanino, K. Takahashi, M. Kato, and T. Yao, Solid State Commun. **65**, 643 (1988).

[14]W. Bacsa (private communication).

[15]M. Tanaka and S. Kurita, J. Phys. Soc. Jpn. **19**, 3019 (1986).

[16]M. Tanaka, S. Kurita, M. Haruki, and M. Fujisawa, Synth. Met. **21**, 103 (1987).

[17]S. D. Conradson, R. F. Dallinger, B. I. Swanson, R. J. H. Clark, and V. B. Croud, Chem. Phys. Lett. **135**, 463 (1987).

[18]M. Haruki (private communication).

[19]M. Sakai, N. Kuroda, and Y. Nishina, Phys. Rev. B **40**, 3066 (1989).

[20]Y. Onodera, J. Phys. Soc. Jpn. **56**, 250 (1987).

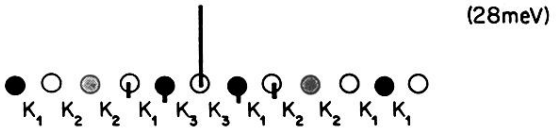

FIG. 10. Eigenstate of the localized gap mode for the Pt-Cl chain with a positive charged soliton; please note the spring force constants distribution used for the fit (within brackets, the calculated eigenvalue).

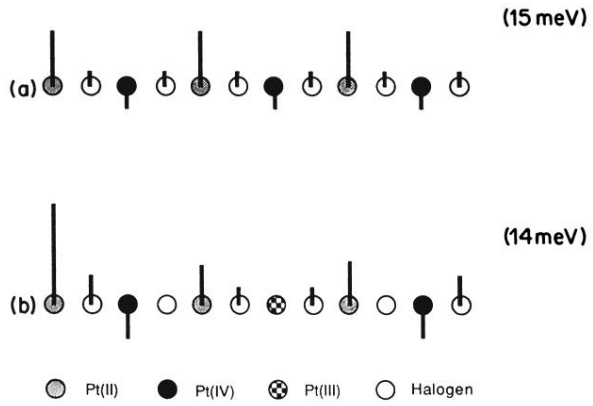

FIG. 3. Eigenstate of the acoustic mode for the Pt-Cl chain (a) without and (b) with a polaron defect (within brackets, the calculated eigenvalue).

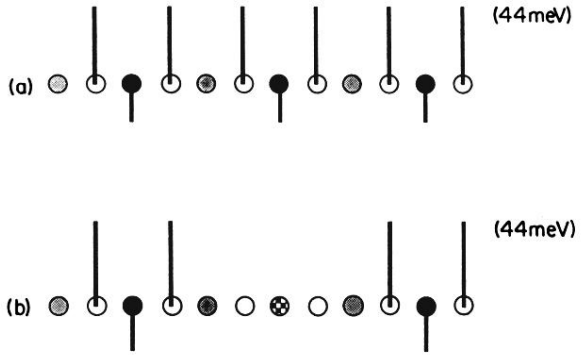

FIG. 4. Eigenstate of the stretching mode for the Pt-Cl chain (a) without and (b) with a polaron defect (within brackets, the calculated eigenvalue).

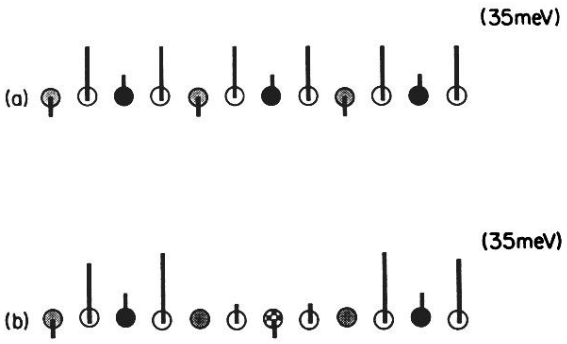

FIG. 5. Eigenstate of the ir-bending mode for the Pt-Cl chain (a) without and (b) with a polaron defect (within brackets, the calculated eigenvalue).

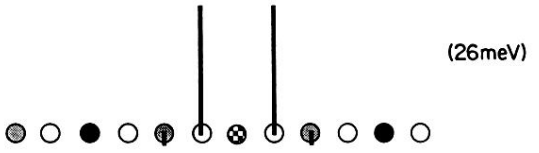

FIG. 6. Eigenstate of the gap mode for the Pt-Cl chain with a polaron defect (within brackets, the calculated eigenvalue).

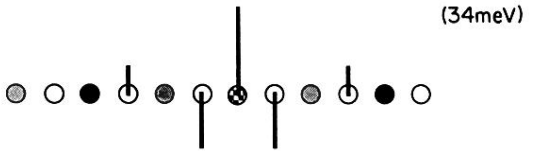

FIG. 7. Eigenstate of the localized bending mode for the Pt-Cl chain with a polaron defect (within brackets, the calculated eigenvalue).

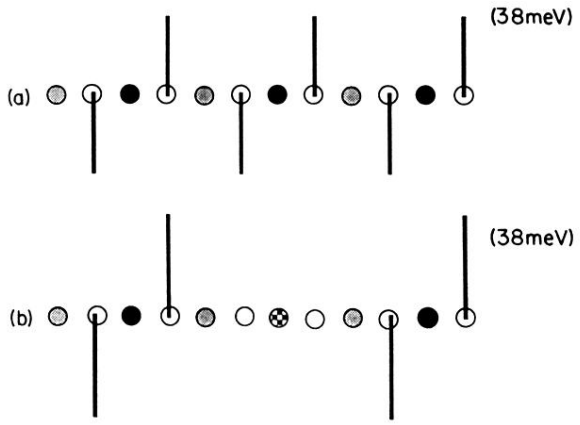

FIG. 8. Eigenstate of the Raman breathing mode for the Pt-Cl chain (a) without and (b) with a polaron defect (within brackets, the calculated eigenvalue).

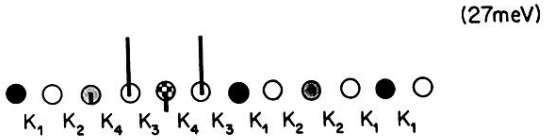

FIG. 9. Eigenstate of the localized gap mode for the Pt-Cl chain with a neutral soliton; please note the spring force constants distribution used for the fit (within brackets, the calculated eigenvalue).